

PAPER • OPEN ACCESS

On the 3D structure of the flow-field in the vicinity of inclined plate

To cite this article: P Prochazka *et al* 2018 *J. Phys.: Conf. Ser.* **1101** 012026

View the [article online](#) for updates and enhancements.



IOP | ebooks™

Bringing you innovative digital publishing with leading voices to create your essential collection of books in STEM research.

Start exploring the collection - download the first chapter of every title for free.

On the 3D structure of the flow-field in the vicinity of inclined plate

P Prochazka¹ and V Uruba^{1,2} and V Skala¹

¹Institute of Thermomechanics, Czech Academy of Sciences, Dolejškova 5, Praha 8, Czech Republic

²University of West Bohemia, Faculty of Mechanical Engineering, Department of Power System Engineering, Universitní 8, Plzeň, Czech Republic

prochap@it.cas.cz

Abstract. The motivation of the presented study is supporting new ideas about principle of flight by Hoffman and Johnson, see [1]. The new hypothesis of physical mechanism of flight relies on existence of streamwise vortical structures on the suction side of the airfoil and within its wake. The vortices origin is supposed to be the instability of the boundary layer subjected to adverse pressure gradient. The vortices are of highly dynamical nature, changing their position, size and other parameters in time very rapidly. For this experiment the simplest airfoil possible was chosen represented by a flat plate in uniform flow and moderate angle of attack. In the suggested paper detailed measurement of the zone of interest will be carried out using stereo PIV method. System of measuring planes perpendicular to the flow will be explored. POD analysis is to be utilized.

1. Introduction

The generation of the lift seems to be resolved issue in the community of people dealing with the aerodynamics. Nevertheless, the traditional Newton mechanics did not give an answer how the lift (and also drag) is created. For example, potential flow for incompressible flow gives zero drag and also lift (D'Alembert's Paradox). Kutta-Zukovskij equation uses an auxiliary variable (circulation) to simulate the lift. The circulation is however unphysical and it was not observed in the nature. To uncover the secret of flight D'Alembert's Paradox should be resolved. The true physical principal of lift and flight has been investigated (experimentally and numerically) by authors Hoffman and Johnsson [1, 2]. They formulated some new ideas - the downwash effect is a necessary condition to generate the lift and the downwash is coming from a low-pressure rotational slip separation. So the main source of the lift generation should be the existence of the streamwise vortical structures located above the wing and in the wake behind it. The streamwise vorticity is presented as a consequence of the natural instabilities of the boundary layer developing under adverse pressure gradient on the airfoil suction side. Some experiments of flow instabilities and their effects were presented recently [3, 4].

This experimental study is dealing with streamwise-oriented vortical structures investigated in parallel planes around and behind the simplest case of the airfoil – flat plate with semi-cylindrical edges. Previous study within this research were oriented both on streamwise vorticity behind the plate [5] and on the investigation of the boundary layer in suction side [6]. Presented study focuses on detailed investigation in several parallel planes perpendicular to the incoming flow using stereo PIV technique (2D3C approach). The flow field is studied not only in the wake and suction side but also the pressure side is examined. The downwash effect is fully detectable as well as streamwise vortices which are characterized by highly dynamical nature, rapid changes of their positions, size and other parameters. The dynamic flow is decomposed using POD (Proper Orthogonal Decomposition) into most dominant flow structures taking effect on this phenomenon.



This article contains preliminary results from just one type of measuring planes (fig. 1). Another articles will be presented concurrently and in the future for parallel planes with the wing surface and also for 2D3C vector field in the perpendicular planes to currently one used.

2. Experiment description

2.1 Model geometry

The test model of simple flat plate with semi-cylindrical leading and trailing edges was placed in a uniform low turbulence stream. The stream was produced using blow-down wind tunnel situated in the Laboratory of turbulence and shear layers. The distribution of velocity was perfect uniform, intensity of turbulence was under 0,2% and the flow was perfect steady in time for the incoming velocity 5 m/s. The plate was inclined at the angle of attack 7° with respect to the channel flow. (The pressure side of the profile was measured for AoA -7° due to technical reasons). The span dimension of the airfoil is 450 mm, the chord length is $c = 100$ mm and the thickness is 2 mm. Corresponding Reynolds number is about 33 000.

The schematic view of the experimental layout is plotted in figure 1. There is a rotatably mounted wing just behind the wind tunnel nozzle with cross-section dimension 250 x 250 mm. The Cartesian coordinate system was introduced so that the origin was located in the middle of the trailing edge. The x- and y-axis are in the plane of measurement and z-axis is oriented perpendicular to the FoV (field of view) with the direction of stream. There are three green parallel planes in the airfoil wake at dimensionless positions $z/c = 0.5, 1$ and 1.5 . Finally, twenty distinct measuring planes (7 upstream the trailing edge and 13 downstream) were investigated with the distance between two adjacent planes 10 mm. This gave us quite good image about flow field topology of flow domain. The trailing edge position is characterized by the rate $z/c = 0$.

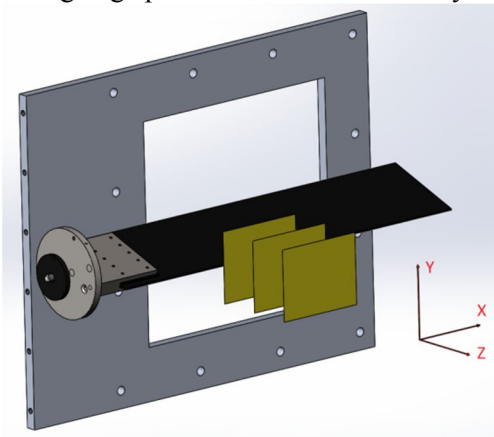


Figure 1. The setup of inclined plate and wind tunnel orifice, $z/c = 0.5, 1$ and 1.5 .

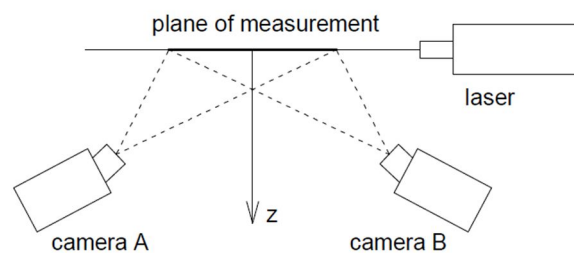


Figure 2. Stereo PIV layout.

2.2 Measurement technique

All three velocity component of each individual measuring planes were detected using stereoscopic time-resolved PIV technique. The measuring apparatus is from Dantec company. The laser New Wave Pegasus, Nd:YLF double-head, was used to illuminate the safex particles. It emits the coherent light with wavelength of 527 nm, maximal frequency is 10 kHz, shot energy is 10 mJ (for 1 kHz) and corresponding power is 10 W per head. Two CMOS cameras NanoSense MKIII with Scheimpflug mounting of lenses were used to capture the tracing particles distributed in the flow. Each camera has resolution of 1280 x 512 pixels, maximal corresponding acquisition frequency is 512 double-snaps per second. The dimensions of FoV was 100 x 60 mm. The data acquisition was conducted in Dynamic Studio software ver. 3.4. Preceding calibration was performed using standard calibration target 100 x 100 mm. The shifting in z-direction was precisely performed by stepper motor in five positions (-2, -1, 0, 1, 2 mm). The calibration (Pinhole camera model) error was set to approx. 0,2 pixels. The 3-component vel. vector field was consequently evaluated and each plane was created by 99x61 vectors. Further analysis was performed in newer version of this software 6.2. The schematic view of stereo PIV layout is in figure 2.

2.3 POD analysis

The typical way, how to apply decomposition methods POD is on two-dimensional dataset. In the presented article, the POD will be applied for three-component vector fields gained from stereo PIV anemometry. POD analysis is used here to extract the most energetic dominant coherent structures presented in the random turbulent flow. This analysis is coming from the vel. fluctuations which means that the mean value is subtracted from all snapshots. The number of resulting orthogonal topological POD modes is equal to number of all PIV snaps. The detailed information about POD calculation can be seen e.g. in [7]. The result is a set of POD mode ordered according to the relative kinetic energy content. Low order modes (high-energy) contain the most dominant flow structures. These ones will be investigated above, below and behind the airfoil as well as their evolution in longitudinal direction. This research was dealing with statistical quantities evaluation as well as POD modes. For this purpose, the acquisition frequency of 100 Hz was set as desirable.

3. Results

The presented data were acquired by the TR-PIV system and will be mainly presented in the form of vectors and scalar distribution in the measuring plane xy perpendicular to the channel flow with direction z . Previously, some preliminary investigation of isolated planes behind the plate were acquired. The area above and below the plate surface (suction and pressure side) are emphasized in this article. Generally in this paper, black vectors represent the velocity components projected into the measuring plane xy . The color represents scalar value, e.g. streamwise vel. component W or turbulent kinetic energy (TKE). The black line represents the position of trailing edge (or its projection in the incoming flow direction) and dashed line is used to emphasize the projection of the trailing edge in the direction of the inclined plate (7°). Black streamlines were added to make the instantaneous vortices visible and green lines were used to plot the z -vorticity (ω_z) in the case of POD flow topology.

The results are to be presented in dimensionless form. All coordinates are divided by the chord length $c = 100$ mm. The velocity magnitude is normalized using incoming flow velocity $U_e = 5$ m/s. Turbulent kinetic energy is normalized by U_e^2 .

3.1 Instantaneous velocity

There are presented three distinct measuring planes $z/c = -0.5, 0$ and 0.5 (figure 3) to see how the instantaneous streamwise vortices are evolving along streamwise coordinate z . While the pressure side more or less does not show any strong perturbations, the suction side is full of vortices already in the middle of the plate chord ($z/c = -0.5$). These PIV snapshots show that these structures are irregular, they are changing very rapid in time and in space (they are not regular along x -axis unlike mean image). The vortices are extending in their size in downstream direction ($z/c = 0$) and merging with each other which leads to decreasing of their number and strength ($z/c = 0.5$). The streamlines clearly show downwash effect, the wake position (minimal velocities – blue and green color) is located a little above the dashed projected line. There is impossible to follow the structures snapshot per snapshot with rather low acquisition frequency 100 Hz. That is why, further investigation of these vortices will be provided by POD decomposition.

3.2 Time-mean velocity

Twenty measuring planes were investigated in total (seven of them above and below the profile) which gave us very detailed information about mean flow field topology around the inclined flat plate with AoA 7° . The statistical values were calculated from approx. 1600 PIV snaps measured in 16 seconds. There are plotted isolines of velocity magnitude ($70\% U_e, 80\% U_e$ and $90\% U_e$) in figure 4. The flat plate is displayed in its whole span. The origin of coordinate system is located in the middle of trailing edge. A different representation of acquired results provides figure 5. There one can see all measuring planes and three different distribution of scalar value (velocity modulus, TKE and V -component). Notice, that the distribution is not dependent on x -axis. The flow seems to be 2D from these results. However inst. images have revealed fully three-dimensional behaviour of the flow. Maximal velocities (higher than $100\% U_e$) are located just behind the leading edge (very first plane) - a small separation bubble was detected further upstream during other experiments. This clear velocity overshoot is locally oriented, further downstream the maximal velocities does not exceed U_e . The

formation of wake region is clearly seen as well as downwash angle. Maximal TKE values, which characterize locally dynamic activity, can be observed above the plate. The fluctuation activity takes a half value in the wake region. Notice, the TKE is almost negligible in the region of pressure side.

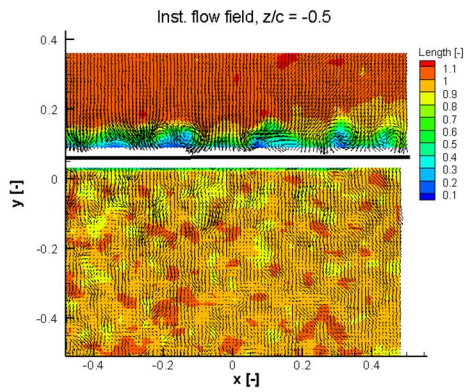


Figure 3a. Instantaneous vel. vector map for plane $z/c = -0.5$, distribution of velocity length.

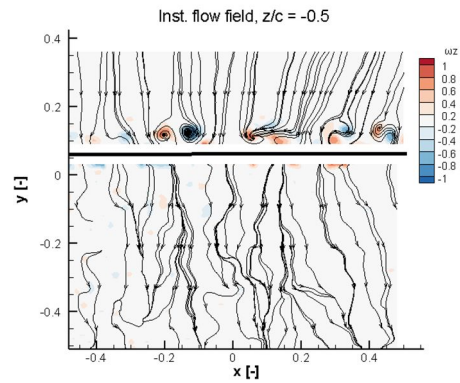


Figure 3b. Instantaneous vel. vector lines for plane $z/c = -0.5$, distribution of vorticity.

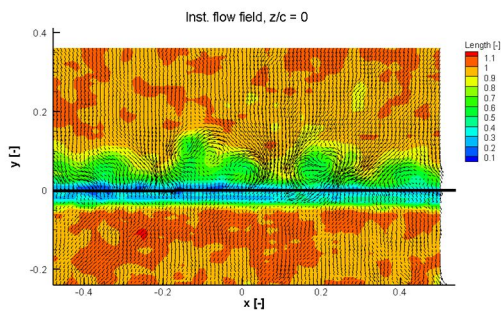


Figure 3c. Instantaneous vel. vector map for plane $z/c = 0$, distribution of velocity length.

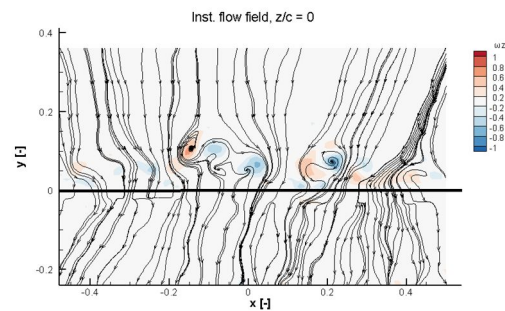


Figure 3d. Instantaneous vel. vector lines for plane $z/c = 0$, distribution of vorticity.

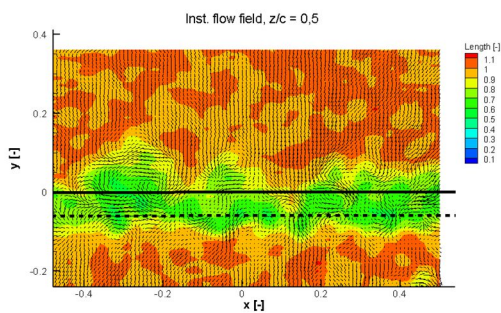


Figure 3e. Instantaneous vel. vector map for plane $z/c = 0.5$, distribution of velocity length.

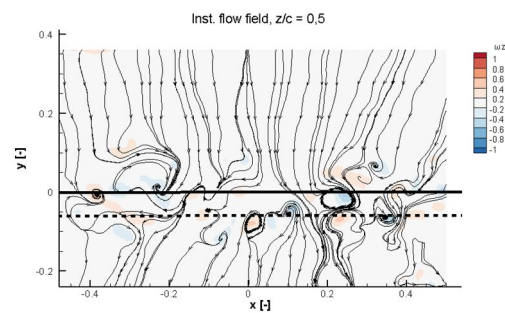


Figure 3f. Instantaneous vel. vector lines for plane $z/c = 0.5$, distribution of vorticity.

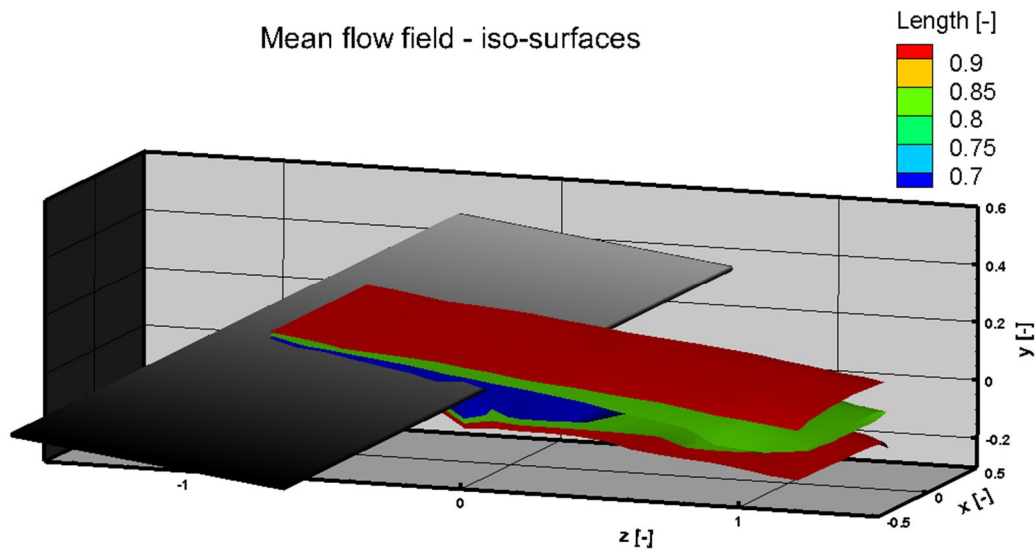


Figure 4. Iso-surfaces of velocity length, time-mean flow field behind inclined plate.

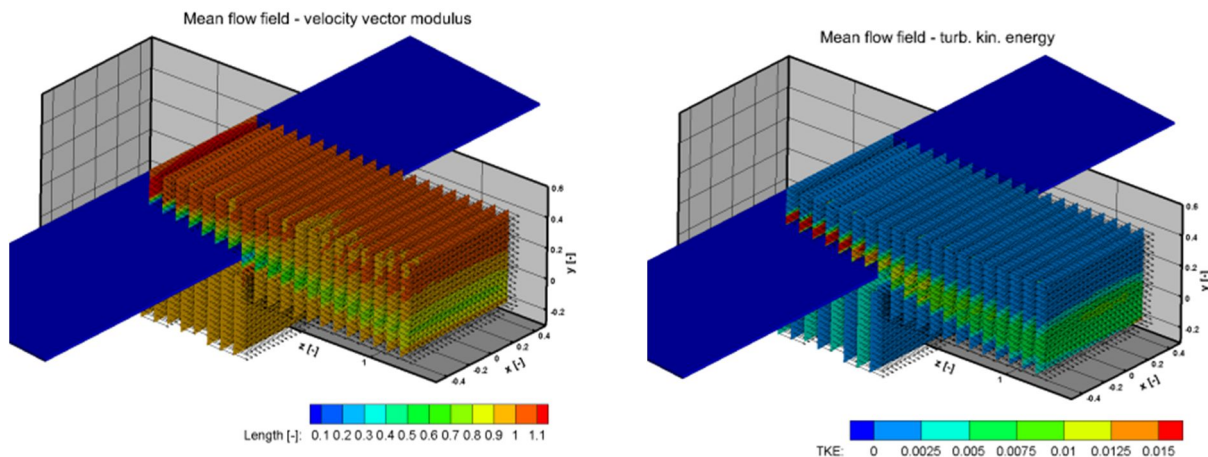


Figure 5a. Time-mean flow, distribution of velocity length in 20 consecutive planes.

Figure 5b. Time-mean flow, distribution of TKE in 20 consecutive planes.

The pressure side did not demonstrate any coherent structures. On the other hand, the velocity evolution is slightly dependent on z -axis (figures 6a,b). The flow is decelerated a little to $90\% U_e$ ($z/c = -0.7$) to be re-accelerated more close to the trailing edge. An obvious increase of the boundary layer thickness along z -coordinate can be seen in suction side. It was not possible to measure so close to the lower surface from some technical reasons nevertheless the boundary layer of pressure side does not reach such extension in thickness. The maximal fluctuation activity at 50% of chord length is situated close to the upper surface ($y = 0.12$). No velocity perturbations were revealed for pressure side. Figure 6d depicts another mean flow field evolution further downstream in the wake ($z/c = 0$). The maximal TKE values are located still slightly above the surface at the plane of the leading edge. The position of the wake center is shifted below with increasing distance from trailing edge.

The minimum is located near the dashed line (this is valid for all investigated planes). This implies that the downwash angle should be close to the AoA. This is valid but only for narrow region inside the wake. Figure 7 shows the distribution of v -velocity component in all domain. The green color corresponds to approx. 10% of U_e and blue is even higher - 15%. Biggest value (more than 7°) is above the plate and near the leading edge. On the contrary the smallest value was detected in the pressure region where the value is 5° . In the wake in substantial distance from the trailing edge, the downwash effect becomes weaker. The downwash effect is nicely seen in figure 8 where the zy plane is reconstructed.

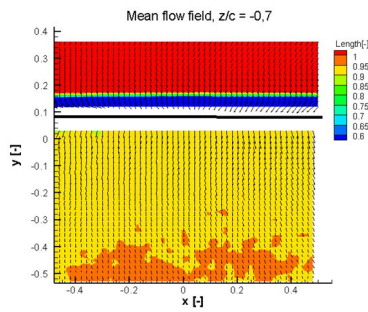


Figure 6a. Velocity distribution for suction and pressure side in $z/c = -0.7$.

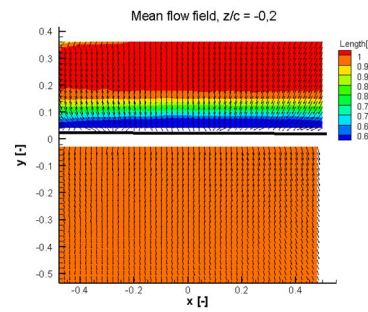


Figure 6b. Velocity distribution for suction and pressure side in $z/c = -0.2$.

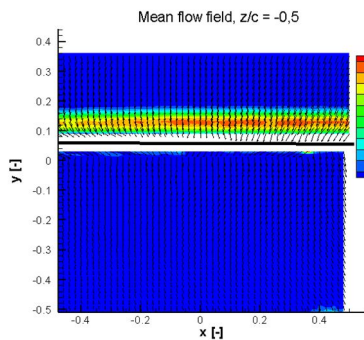


Figure 6c. Distribution of TKE for both side in $z/c = -0.5$.

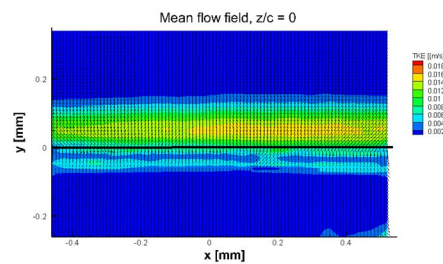


Figure 6d. Distribution of TKE for both side in $z/c = 0$.

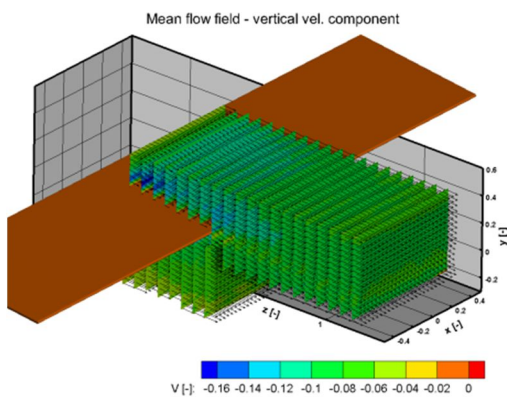


Figure 7. Time-mean flow, distribution of vertical velocity in 20 consecutive planes.

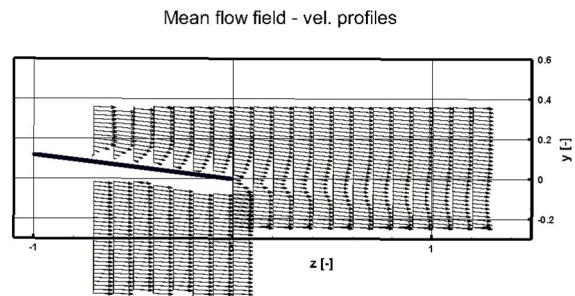


Figure 8. The effect of downwash to vector field.

3.3 POD modes

POD is a great tool to identify most relevant vortex structures from turbulent flow field containing significant coherent structures. Although the highest-order modes represent very often only noise, all 1600 modes were valuated. It is possible to reconstruct the whole flow field around the airfoil using modes recombination. The second POD mode, which is characterized by the existence of one pair of contra-rotating vortices, was selected to reconstruct one of the possible forms of the flow field. The figure 9 shows two vortex cores (detected by negative and positive vorticity). The inclination due to the flate plate is about 1° smaller. This effect can also be seen from other types of modes, e.g. at the plane $z/c = 0.8$. Figure 10 is plotted for other two types – 7. and 16. modes and they are characterized by the existence of three pairs and several pairs of streamwise vortices. The location of them is situated slightly above dashed line (the projection of trailing edge in the incoming flow direction). Moreover the second plotted mode contents the structures that are also placed below. The green lines

are isolines of vorticity (positive or negative) and the space between two adjacent vortices are filled by the accelerating or decelerating fluid (streaks). The vortices are located in the centers of isolines.

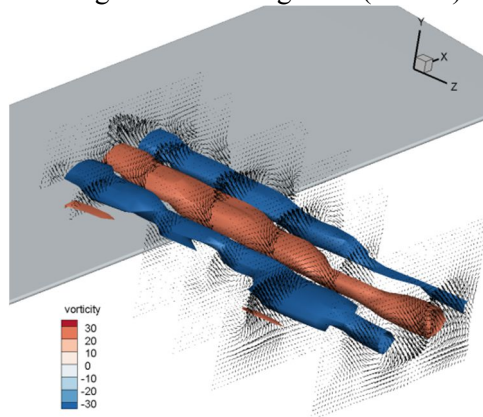


Figure 9. The reconstruction of two counter-rotating streamwise-oriented vortices in the airfoil wake. One of the conceivable form of the flow field.

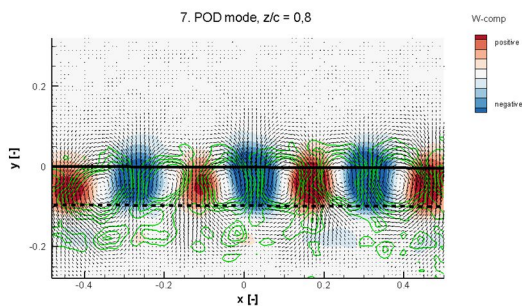


Figure 10a. 7th POD mode in $z/c = 0.8$ in the form of three pairs of counter-rotating vortices.

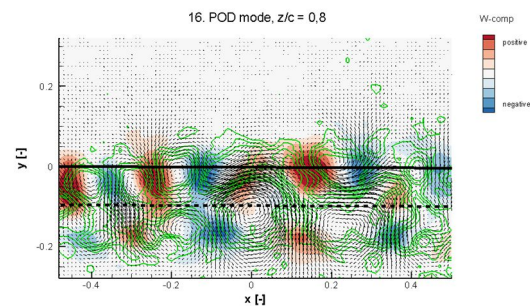


Figure 10b. 16th POD mode in $z/c = 0.8$ in much complex form, vortices also below dashed line.

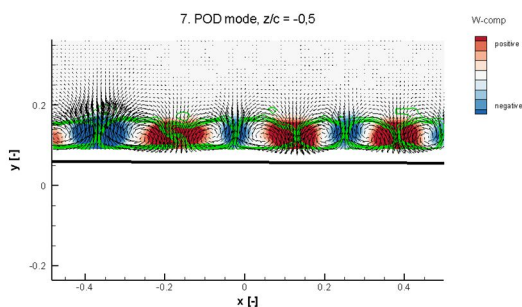


Figure 11a. 7th POD mode in $z/c = -0.5$ for suction side.

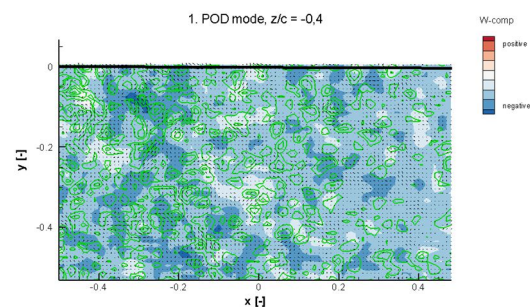


Figure 11b. First POD mode in $z/c = -0.4$ for pressure side, orderly smaller amplitudes.

The suction side is the place where one can find the origin of these structures. Figure 11a is plotted for seventh POD mode in $z/c = -0.5$ which is characterized by the existence of vortex pairs located very close to the airfoil surface. Their distribution is perfect regular. We can decompose similar modes revealing streamwise vortices in downstream direction, but there were not detected such structures closer to the leading edge. From TKE distribution, it is obvious that there is no strong dynamics in pressure side. This corresponds with the first mode evaluated at $z/c = -0.4$ below the airfoil. One cannot see any velocity streaks and even this is the high-energy mode, there are no dominant coherent structures (very low amplitude). Little importance of POD mode in pressure side considering to suction side is visible at the table 1. Sum of ten first mode contain only 5% of energy for pressure side unlike 30% for suction side at $z/c = -0.5$. Fifty first modes contain more than 2/3 of total energy for suction side unlike 16% of energy for pressure side.

The relative energy content of first twenty modes for both side are compared in graph 12. Especially first five suction modes are dominating over pressure modes. Figure 12b illustrates the

development along z-coordinate. POD modes evaluated in measuring planes corresponds to the trailing edge position contain slightly more kinetic energy than modes located more downstream.

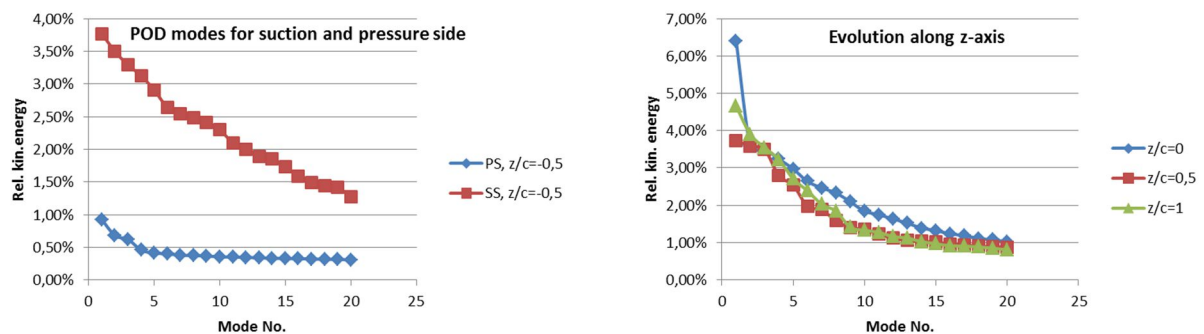


Figure 12a. The importance of 20 POD modes for pressure (blue) and suction sides.

Figure 12b. Rel. kin. energy content of 20 POD modes along streamwise coordinate.

Table 1. Kinetic energy fraction, the comparison of pressure and suction sides.

	Pressure side			Suction side		
	$z/c = -0.5$	$z/c = -0.3$	$z/c = -0.1$	$z/c = -0.5$	$z/c = -0.3$	$z/c = -0.1$
10 modes	4,96%	4,40%	5,35%	28,96%	31,47%	32,52%
20 modes	8,24%	7,73%	8,61%	45,74%	47,88%	48,25%
50 modes	16,50%	16,21%	16,89%	67,25%	68,37%	68,19%

4. Conclusion

The experimental evaluation of streamwise vortices was done. The downwash effect was depicted in detail and downwash angle was set for various flow domain location. Rotational slip separation was studied in the trailing edge location as well as the vortices origin was investigated close to the leading edge. No relevant velocity disturbances were found at pressure side. Low-order POD modes imply that the flow is based on the existence of streamwise vortices above the plate and in the wake and that these structures are subjected to the downwash effect. Both findings support a new theory of flight and lift generation [1].

References

- [1] Hoffman J and Johnsson C 2009 The Mathematical Secret of Flight *Normal 57*, Vol.4
- [2] Hoffman J and Johnsson C 2010 Resolution of d'Alambert's paradox *J. Math. Fluid Mech.*, 12(3)
- [3] Uruba V 2016 Force Interaction of an Airfoil in Fluid-Flow *ES 2016*, 7375
- [4] Uruba V 2016 On Aerodynamics Forces Physical Mechanism *SKMTaT 2016*
- [5] Uruba V, Pavlík D, Procházka P, Skála V and Kopecký V 2017 On 3D flow structures behind an inclined plate *EPJ Web of Conferences*, vol 143 Article number 02137
- [6] Uruba V, Procházka P and Skála V 2017 On 3D Flow Structures of the Boundary Layer on the Suction Side of a Plate *EPJ Web of Conferences*, vol 180 Article number 02112
- [7] Uruba V 2012 Decomposition methods in turbulent research *EPF Web of Conferences*, vol 25 Article number 01095

Acknowledgement:

The authors gratefully acknowledge financial support of the Grant Agency of the Czech Republic, project No. 17-01088S.